Skeletal Radiol (1998) 27:352–358

ARTICLE

D.L. Janzen
S.E. Aippersbach
P.L. Munk
D.F. Sallomi
D. Garbuz
J. Werier
C.P. Duncan

Three-dimensional CT measurement of adult acetabular dysplasia: technique, preliminary results in normal subjects, and potential applications

D.L. Janzen, M.D. (✉)
S.E. Aippersbach, M.D.
P.L. Munk, M.D., C.M.
D.F. Sallomi, M.B., Ch.B.
Department of Radiology,
Vancouver Hospital
and Health Sciences Centre,
and University of British Columbia,
855 West 12th Avenue, Vancouver, BC,
Canada V5Z 1M9

D. Garbuz, M.D. · J. Werier, M.D.
C.P. Duncan, M.B., Ch.B.
Department of Orthopedic Surgery,
Vancouver Hospital and Health Sciences
Centre, and University of British Columbia,
Vancouver, BC, Canada

Abstract *Objective.* To assess a three-dimensional computed tomography (3DCT) technique for measurement of acetabular coverage in adults.
Design. We used 3DCT to define the geometric centre of the femoral head and to measure centre-edge angles (CEAs) at 10° rotational increments around the acetabular rim. The means, ranges, standard deviations and 95% confidence intervals for the CEAs at the various rotational increments were determined. Inter- and intra-observer variability was measured. The normal values are compared with two example cases of acetabular dysplasia.
Patients. The normal hips of 15 subjects aged 19–49 years (mean 34.2 years) were measured.
Results. The 3DCT measurements are reproducible (mean difference inter-observer, 1.7°–7.9°; mean difference intra-observer, 0.6°–6.9°). Mean normal CEA at the lateral rim was 33° with a 95% confidence interval of 23°–43°. Mean normal CEAs at 10° rotational increments from anterior to posterior rim were determined, and graphed as a 'normal curve'.
Conclusion. This new 3DCT method of assessing acetabular dysplasia is simple, reproducible, and applicable to diagnosis, quantification and surgical planning for adult acetabular dysplasia patients.

Key words Acetabular dysplasia · Hip dysplasia · Centre-edge angle · 3D computed tomography

Introduction

Accurate measurement of acetabular coverage of the femoral head is desirable for diagnosis of acetabular dysplasia, and for planning of acetabular osteotomies to improve acetabular coverage. Traditionally, acetabular dysplasia in adults has been qualitatively assessed using plain radiographs. A number of quantitative measurements derived from plain radiographs are widely used in clinical practice. These include the centre-edge angle (CEA) of Wiberg as assessed on the anteroposterior radiograph and the 'false profile' radiograph of Lequesne and DeSeze [1–3]. The CEA of Wiberg assesses the lateral coverage of the acetabulum, and the CEA measured on a 'false profile' view is thought to assess the enterolateral coverage of the acetabulum. However, all plain radiographic techniques are limited by superimposition of bony structures and lack of three-dimensional information. While plain films allow a diagnosis of dysplasia to be made, accurate quantification of the degree and location of dysplasia can be difficult. Mathematical estimations of acetabular coverage have been derived from anteroposterior radiographs; however, these methods are complex and require a number of assumptions regarding the geometry of the hip joint [4].

It is well established that three-dimensional CT (3DCT) techniques produce accurate visualization of bony anatomy, and allow accurate angular and linear measurements in an infinite variety of planes [5, 6]. We have devised a simple and reproducible 3DCT technique for the measurement of acetabular coverage in adults. The purpose of this paper is to define the imaging and mea-

surement technique, and to present normative and reliability (inter-observer and intra-observer variability) data. This new technique has a potential clinical role in diagnosis and quantification of acetabular dysplasia, and in planning of rotational acetabular osteotomies.

Materials and methods

The normative data were derived from 15 normal hips in 12 subjects aged 19–49 years (mean 34.2 years). Ten men and two women, and nine right hips and six left hips, were included. Nine subjects had an acetabular fracture requiring thin-section CT scanning in the contralateral hip, and the simultaneously acquired CT data from the normal hip were used for the purposes of this study. Three patients underwent thin-section CT scanning of the hips for suspected soft-tissue abnormalities; the bony structures were entirely normal and both hips were used for normative data. In all cases there was no history of previous injury or abnormality in the 'normal' hip. CT scanning of volunteers was considered inappropriate in light of the gonadal radiation dose of thin-section CT examination of the hips.

The CT scanning was performed using a GE HiLight Scanner (GE Medical Systems, Milwaukee, Wis.). The subjects were positioned supine on the scanning table with the midline of the body aligned with the midline of the scanning table. The legs were fully extended and the feet stabilized in 15° of external rotation. Care was taken to ensure that no pelvic tilt, hip flexion or knee flexion was present. Helical 3 mm CT sections were performed at pitch of 1:1 (120 kV, 300 mA, field of view 38–42 cm, standard algorithm) through the acetabula and femoral heads. The helical CT data were reconstructed at 1-mm intervals.

The scan data were transferred to a 3D workstation (Advantage Windows Workstation, GE Medical Systems). Using the automated 3D bone reconstruction program, a surface-shaded 3D model of the pelvis was obtained. This 3D program automatically discards all soft-tissue attenuation material and produces a surface-shaded image of the bony structures. A cursor was manually deposited at the centre of the femoral head (assuming a spherical contour of the femoral head), using simultaneous viewing of axial, coronal and sagittal images. Vertical planar images were then obtained through the centrepoint of the femoral head at various rotations from 0° (anterior acetabular margin) through 90° (lateral acetabular margin) to 180° (posterior acetabular margin). The CEA was measured at 10° rotational increments around the acetabular rim. The acetabular margin was defined as the edge of the smooth subchondral bone surface. Figures 1 and 2 give a detailed description of the measurement technique.

The means, standard deviations, ranges and 95% confidence intervals of the CEAs at the various positions around the acetabular margin were calculated. Assuming a normal Gaussian distribution, the 95% confidence intervals were calculated. Intra-observer and inter-observer variability was assessed using two repeated observations (on different days) of three different hips by two observers. Note that the assessment of a single hip entails 19 CEA measurements; two assessments each of three different hips by two observers provided a total of 228 CEA measurements that were used for determination of observer variability. The intra- and inter-observer variations were calculated in terms of mean difference in measured CEA.

The data are presented as a graph, with the CEA on the *y*-axis and the rotational position on the *x*-axis (Fig. 3, 4). To allow assessment of global and regional dysplasia severity, 'dysplasia indices' were quantified. The dysplasia indices are based on the area under the curve on a graph of CEA versus position along the acetabular rim. The indices are calculated as a ratio (dysplastic hip/normal mean data). *Global coverage* was defined as the area under the curve from 0° to 180° rotational positions, *anterolateral coverage* from the 0° to 4° positions, *lateral coverage* from the 50° to 120° positions, and *posterolateral coverage* from the 130° to 180° positions.

Results

The means, ranges, standard deviations (SD) and 95% confidence intervals of the CEAs from the 0° (anterior rim) to the 180° position (posterior rim) are presented in Table 1. The distribution of measured CEAs in the study group is shown in Fig. 3. Figure 4 shows the mean and 95% confidence interval at each rotational position around the acetabular rim. A narrow range of normal values for acetabular coverage is present along the anterior and lateral aspects of the acetabulum, with a 95% confidence interval of 53°–69° anteriorly and 23°–43° laterally. The normal ranges widens along the posterior acetabulum (e.g. 85°–123° for posterior coverage). Figure 3 shows a slightly skewed distribution of the normal CEAs around the lateral acetabular rim, with most values clustered near the lower range of normal and most outliers lying in the upper range. This suggests a more tightly defined lower limit of normal and a more variable upper limit of normal for lateral acetabular coverage. CEAs along the anterior and posterior acetabular margins followed a more Gaussian distribution.

The intra- and inter-observer variability are shown in Table 1. Intra-observer and inter-observer variability ranged from 0.6° to 3.1°, and from 1.7° to 3.7°, respectively, along the anterolateral portions of acetabular margin; variability was somewhat larger in the posterior acetabulum (up to 6.9° intra-observer and 7.9° inter-observer). This degree of variability is small and within the range of precision required by the surgical team to plan, execute and measure corrective osteotomies.

The 3DCT measurement technique was simple to learn (learning time approximately 15 min) and relatively rapid to perform (approximately 15 min per hip).

For illustrative purposes, CEAs from two dysplastic hips were obtained using this technique; Fig. 5 compares these CEAs with the mean normal values. The anterior and lateral acetabular deficiency in "dysplastic 2" is easily appreciated. The angular correction at osteotomy needed to normalize coverage at any point is simply the difference between the normal and dysplastic CEAs at that point along the curve. For example, at the 90° position (lateral acetabular margin), the difference between the normal hip (35°) and the dysplastic hip (10°) is 25°; anteriorly (0° position), the difference if 50° (60° minus 10°). At acetabular osteotomy, anterior rotation of 50° and lateral rotation of 10° of the acetabulum would optimize coverage in this patient. In this fashion, our method of acetabular measurement is directly applicable to surgical planning for patients with acetabular dysplasia.

The dysplasia indices provide quantification of global and regional acetabular deficiency. For example, the indices for "dysplastic 1" (Fig. 5) are: global index, 0.61; anterolateral index, 1.0; lateral index, 0.57; and posterolateral index, 0.40. These indices summarize the graphic data and indicate that "dysplastic 1" has global deficiency of ap-

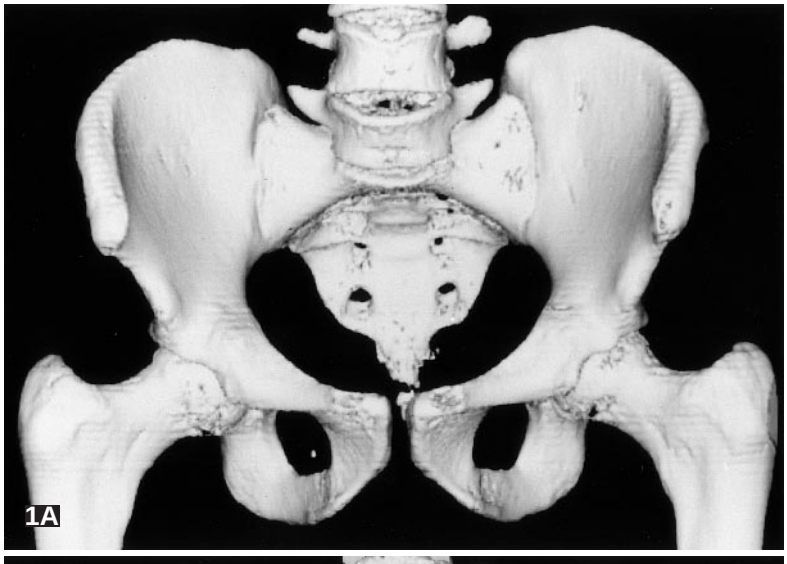
1A


1B

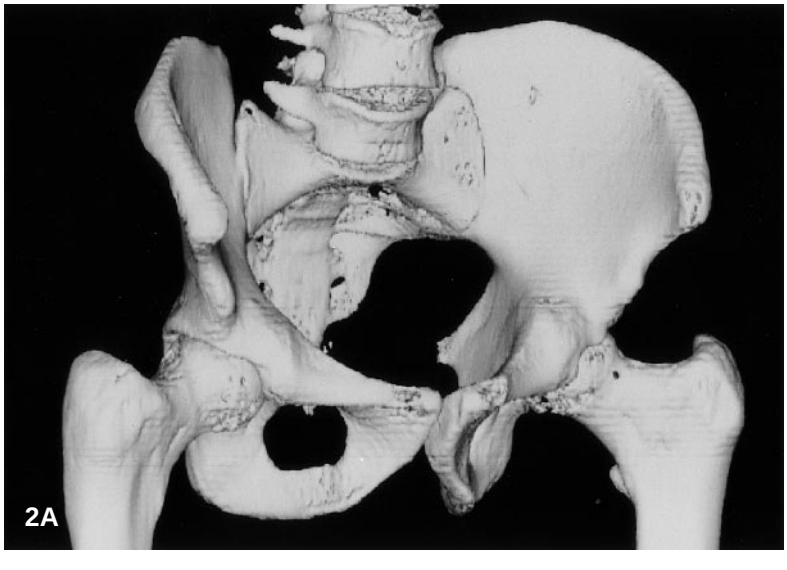
2A

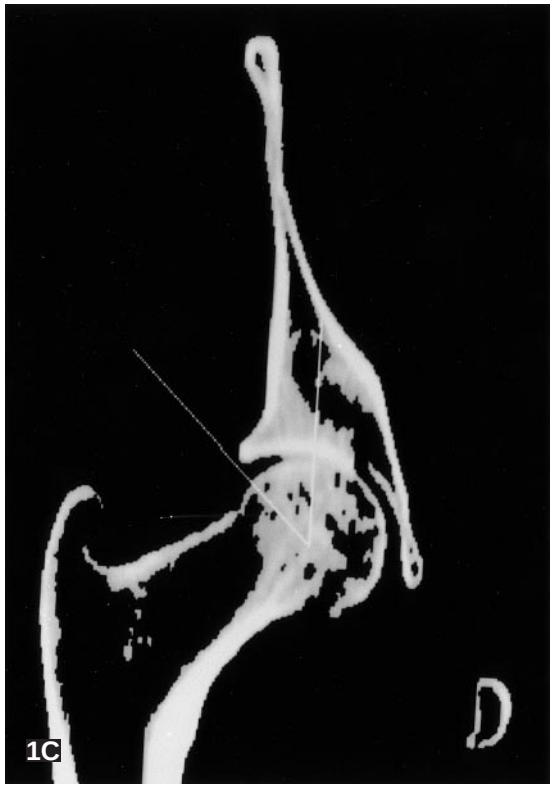
1C
D


2B

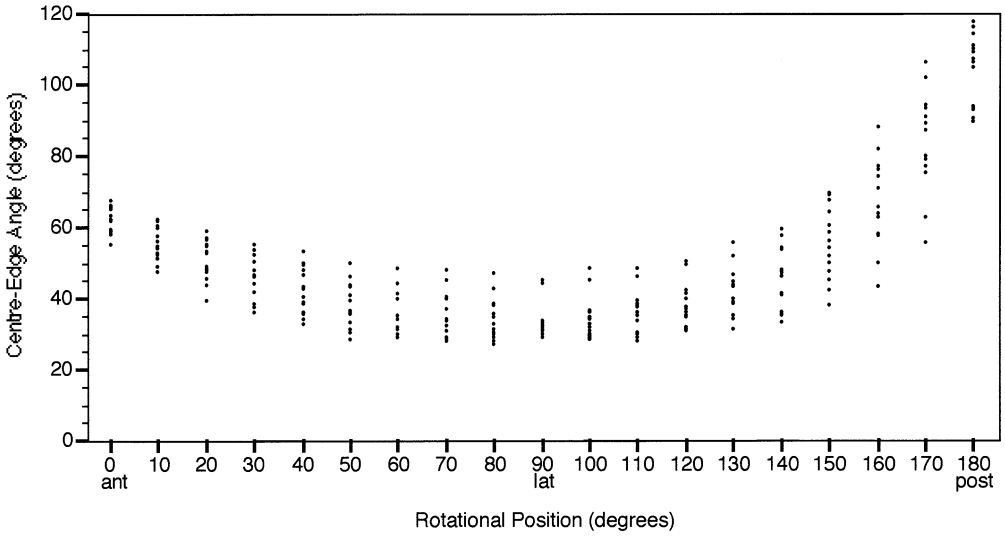

Fig. 3 Scatter plot of the CEAs from 15 normal hips

proximately 40%, with the deficiency located in the lateral and posterolateral portions of the actabulum. "Dysplastic 2" (Fig. 5) has indices of: global index, 0.47; anterolateral index, 0.19; lateral index; 0.31; posterolateral index, 0.75. This hip is more globally deficient than "dysplastic 1" but the uncoverage is predominantly anterolateral and lateral. The dysplasia indices can therefore be used to summarize global and regional acetabular deficiency, and allow easy comparison between patients as well as easy comparison of preoperative and postoperative acetabular coverage.

Discussion

A number of methods have been devised for detection and quantification of acetabular dysplasia in adults. Plain radiographs have traditionally been, and probably remain, the primary imaging modality for both detection and quantification. At least two recent patient outcome studies after innominate or acetabular osteotomy [7, 8] have relied solely on indices obtained from the frontal radiograph (CEA, acetabular angle and percentage femoral head coverage) to quantitatively evaluate preoperative dysplasia and postoperative results. Anteroposterior radiographs of the pelvis do provide reasonable visualization of the lateral acetabular coverage, as defined by the centre-edge angle of Wiberg [1, 2]. The anterior acetabular coverage can be estimated by oblique views of the anterior aspect of the hip [9]. The plain radiographic techniques provide a resonable qualitative assessment of acetabular coverage; however, quantification is severely limited by lack of three-dimensional information and overlap of bony structures on plain radiographs.

A recent report by Konoishi et al. [4] described estimation of three-dimensional acetabular coverage using only an anteroposterior radiograph of the hip. This technique assumes that the acetabulum and femoral head are spherical and congruent, and is very susceptible to errors produced by alterations in positioning and X-ray beam divergence. The technique is also very complex and time-consuming, and requires computer equipment and image digitizers not commonly available in hospital departments. It does not appear well suited to routine clinical use.

CT is an ideal modality for assessment of acetabular coverage, as it provides three-dimensional information with high spatial resolution [5, 6, 10, 11]. CT-based measurements of acetabular coverage have been described by Klaue et al. [3] and Murphy et al. [12]. The method of Klaue et al. [3] involves tracing the acetabular cartilage and femoral head on multiple axial images. The overlapping contours are analysed by a 3D graphics computer program that provides a three-dimensional reconstruction of hip joint cartilage. The apparent limitations of this

◀ **Fig. 1A–C** Measurement of the centre-edge angle (CEA) at the 90° position (lateral acetabular margin) of the right hip. **A** Anterior view of a three-dimensional CT (3DCT) surface-shaded model of a human pelvic phantom. A phantom was used in these figures so that the entire pelvis could be displayed for illustrative purposes. **B** A coronally oriented cut plane through the centre of the femoral head is obtained. The femoral head centre is located by simultaneous viewing of axial, sagittal and coronal sections through the pelvis (not shown). **C** Coronal planar image through centre of the right femoral head. This corresponds to the cut plane in **B** above. The CEA is measured as the angle between the vertical axis and the line connecting the femoral head centre to the lateral acetabular margin. Our 90° position corresponds directly to the classical CEA of Wiberg on the frontal radiograph

Fig. 2A, B Measurement of the CEA at the 120° position of the right hip. **A** The 3DCT model has been rotated 30° right anterior oblique. A cut plane (not shown) is taken through the centre of the right femoral head, as in Fig. 1B above, now running obliquely relative to the pelvis: the cut plane lies in the same plane as this photograph. **B** The resultant planar image at this rotation. The CEA at this rotation is measured. This is an example of how the pelvic model is rotated around a vertical axis to obtain CEAs in 10° increments from anterior acetabular rim (0° position) to lateral rim (90° position), to posterior rim (180° position)

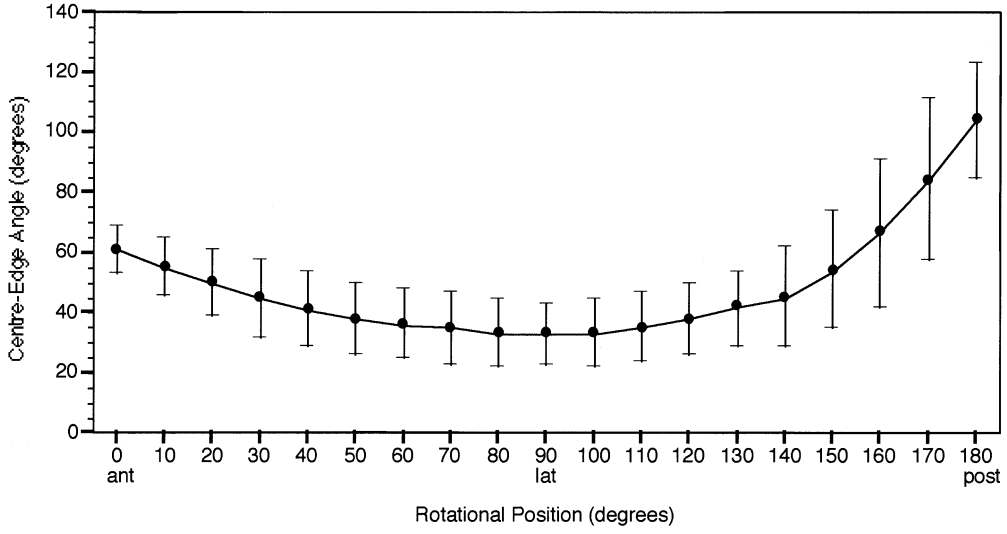

Fig. 4 Mean CEAs and 95% confidence intervals derived from 15 normal hips

Table 1 Centre-edge angle (*CEA*) data from 15 normal hips, and intra- and inter-observer variability from three normal hips (*SD* standard deviation)

Position (deg rotation)	CEA (deg)				Mean difference in CEA (deg)	
	Mean (n=15)	SD (n=15)	Range (n=15)	95% confidence interval (n=15)	Intra-oberserver varicibility (n=3)	Inter-observer varicibility (n=3)
0 (anterior)	61	4.1	55–67	53–69	2.0	2.8
10	55	4.9	47–62	46–65	2.1	2.5
20	50	5.5	39–58	39–61	0.9	3.7
30	45	6.5	36–55	32–58	1.6	2.9
40	41	6.5	32–53	29–54	0.9	1.7
50	38	6.2	28–49	26–50	1.4	2.5
60	36	5.7	29–48	25–48	0.9	2.5
70	35	6.2	28–48	23–47	1.5	1.8
80	33	5.7	27–47	22–45	1.2	3.6
90 (lateral)	33	4.9	28–45	23–43	1.7	3.0
100	33	5.9	28–48	22–45	0.6	1.7
110	35	6.0	28–48	24–47	3.1	3.3
120	38	6.1	30–50	26–50	1.9	2.7
130	42	6.4	31–55	29–54	2.8	3.7
140	45	8.4	33–59	29–62	4.1	4.5
150	54	9.9	38–69	35–74	6.9	4.4
160	67	12.4	43–88	42–91	3.7	6.4
170	84	13.5	55–106	58–111	2.8	6.6
180 (posterior)	104	9.8	89–117	85–123	4.0	7.9

technique include the need for specialized equipment and the time-consuming nature of the analysis. The method of Murphy et al. [12] involves construction of surface contour maps of the acetabular surface and femoral head (derived from axial images), from which the acetabular orientation can be determined and manipulated. Femoral head containment is defined in terms of anterior, lateral and posterior (centre-edge) angles. Note that the anterior and posterior angles are measured in a transverse plane and are not analogous to the centre-edge angle of Wiberg, which is measured in a vertical plane. Anda [13] suggested that the terms anterior and posterior acetabular sector angles should be used, rather than anterior and posterior centre-edge angles. The technique of Murphy et al. 12] appears very time-consuming and also requires specialized computer and graphics equipment.

Our method of CT quantification of acetabular coverage has some distinct advantages. First, the technique is not time-consuming: analysis of a single hip can be done in approximately 15 min with little experience. The technique is also reproducible, with small inter- and intra-observer variability. The equipment required consists of the General Electric Advantage Windows workstation, which is commonly attached to General Electric helical CT

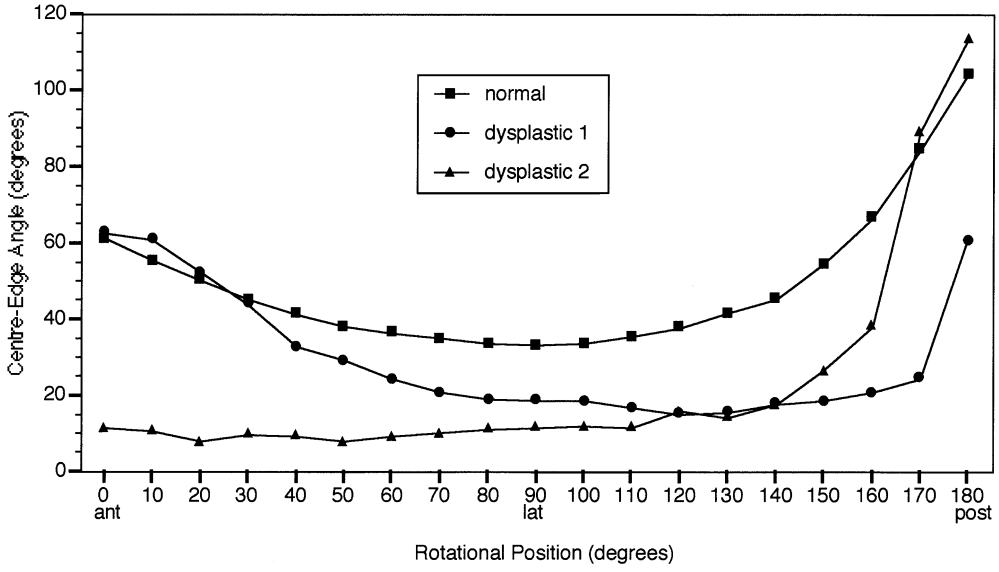

Fig. 5 Comparative plots of CEAs from two dysplastic hips versus mean normal values

scanners. The CT workstations supplied by other equipment vendors may also support this method of analysis. Another advantage of our technique is that the CT results are directly comparable to the plain radiographic findings. The centre-edge angle of Wiberg, as defined on an anteroposterior radiograph, is equivalent to our CEA at the 90° (lateral) position, and the centre-edge angle as measured from a false profile view is equivalent to our CEA at the 90° position.

Our technique also has applicability to surgical planning. There is clearly a significant amount of individual variability among patients with hip dysplasia [3, 12]. It is important, then, to measure and plan the osteotomy on the basis of each patient's unique acetabular anatomy. During osteotomy, the surgeon is able to perform and measure angular reorientation of the acetabulum, thus the measurement technique should assess angular coverage of the femoral head rather than other parameters such as surface area coverage. For instance, the surgeon can reproducibly obtain 10° of mediolateral reorientation of the acetabulum; however, he cannot reliably obtain 5 cm^2 of increased surface area coverage, as the femoral head is not exposed during the surgery. Using our method, the angular coverage of a dysplastic acetabulum can be directly compared with mean normal values (Fig. 5), and the amount of rotation required to normalize the acetabular coverage measured from the graph as the difference between the dysplastic hip and the normal hip at various points along the curve. Intra-operatively, these measurements can then serve as a guide to the surgeon. The use of angular coverage measurements also corrects for variations in patient size, whereas "normal" surface area coverage measurements are difficult to obtain due to the variable size of the femoral head articular surface.

Our technique has a number of important limitations. First is not ideally suited to patients with non-spherical femoral heads, as the centre of the femoral head cannot be defined precisely; this will lead to increased measurement variability. Other previously described techniques also require the assumption of femoral head sphericity [4, 12]. Malalignment of the pelvis on the CT scanner gantry will alter the measurements. While lateral pelvic tilting can easily be controlled by assessing the anterioposterior scout image, the vertical tilt (i.e. lumbosacral lordosis or kyphosis) is difficult to control or measure and may introduce error into our measurements.

Our sample population was relatively small (15 hips) and consisted mostly of men (12 male hips, 3 female hips). However, most adult dysplastic patients are women. Further studies with larger sample sizes will be needed to better define normal acetabular coverage, and to establish whether gender differences exist for acetabular coverage. Finally, there remains concern about the gonadal radiation dose inherent in thin-section CT of the acetabulum, especially as most adult acetabular dysplasia patients are women of child-bearing age. However, no alternative, radiation-free imaging methods are currently available to quantify acetabular dysplasia. MRI may provide a radiation-free method of assessment; however, the bony anatomy is more clearly shown with CT.

In summary, this study describes a new 3DCT technique for acetabular coverage measurement. This method is reliable, reproducible, and simpler than the previously published 3DCT techniques. The technique holds promise for the detection and quantification of acetabular dysplasia, and for surgical planning of acetabular osteotomy and realignment.

References

1. Fredensborg N. The CE angle of normal hips. Acta Orthop Scand 1976; 47: 403–405.
2. Mandal S, Bhan S. The centre-edge angle of Wiberg in the adult Indian population. J Bone Joint Surg Br 1996; 78: 320–321.
3. Klaue K, Wallin A, Ganz R. CT evaluation of coverage and congruency of the hip prior to osteotomy. Clin Orthop 1988; 232: 15–25.
4. Konoishi N, Mieno T. Determination of acetabular coverage of the femoral head with use of a single anteroposterior radiograph. J Bone Joint Surg Am 1993; 75: 1318–1333.
5. Martinez CR, Di Pasquale TG, Helfet DL, Graham AW, Sanders RW, Ray LD. Evaluation of acetabular fractures with two- and three-dimensional CT. Radiographics 1992; 12: 227–242.
6. Kuszyk BS, Heath DG, Bliss DF, Fishman EK. Skeletal 3-D CT: advantages of volume rendering over surface rendering. Skeletal Radiol 1996; 25: 207–214.
7. McCarthy JJ, Fox JS, Gurd AR. Innominate osteotomy in adolescents and adults who have acetabular dysplasia. J Bone Joint Surg Am 1996; 78: 1455–1461.
8. Shindo H, Igarashi H, Taneda H, Azuma H. Rotational acetabular osteotomy for severe dysplasia of the hip with a false acetabulum. J Bone Joint Surg Br 1996; 78: 871–877.
9. Lequesne M, de Seze S. Le faux profile du bassin: nouvelle incidence radiographique pour líetude de la hanche. Son utilité dans les dysplasies et les différentes coxopathies. Rev Rhum Mal Osteoartic 1961; 28: 643–644.
10. Conway WF, Totty WG, McEnery KW. CT and MR imaging of the hip. Radiology 1996; 198: 297–307.
11. Delaunay S, Dussault RG, Kaplan PA, Alford BA. Radiographic measurements of dysplastic adult hips. Skeletal Radiol 1997; 26: 75–81.
12. Murphy SB, Kijewski PK, Millis MB, Harless A. Acetabular dysplasia in the adolescent and young adult. Clin Orthop 1990; 261: 214–223.
13. Anda S. Letter to editor. Clin Orthop 1993; 286: 308–310.